Circuit Breaker Kinematic Analysis

Vivek Sairu Naik[1] and R.K.Tavildar[2]

M.Tech Machine Design Student, Department of Mechanical Engineering, KLS' GIT, Belgaum, Karnataka, India [1]
Assistant Professor, Department of Mechanical Engineering, KLS' GIT, Belgaum, Karnataka, India [2]

ABSTRACT

This project work provides an overview on the common on-site test methods to ensure the safe and reliable operation of circuit breakers used in high and medium-voltage power systems. Failures on circuit breakers can generally be ascribed to defects in one or more of the three main components: The operating mechanism includes mechanical linkage, the electrical control circuits and the components at system voltage. Therefore, determining the energy margin and operational characteristics of the circuit breaker reduces the risk of failures during operation. The on-site testing practices include timing, travel and contact force measurements to assess the integrity of the kinematic chain and control circuits. In addition, characteristics like speed-time curves, bounce, contact travel etc were validated using the CREST system. The system was tested to validate the mathematical model. This paper discusses the optimization of the linkage system using the mathematical model and how to interpret measurement results.

Keywords: Circuit Breaker, Mathematical Model, Energy Margin

1. INTRODUCTION

Circuit breakers are the switching and current interrupting devices. Basically a circuit breaker comprises a set of fixed and movable contacts. The contacts can be separated by means of an operating mechanism. The separation of the current carrying contacts produces an arc. The arc is extinguished by a suitable medium such as dielectric oil, air, vacuum, SF6 gas.

Circuit breakers constitute a critical and important component in the electric power distribution system. Because of their key role in system, circuit breakers are periodically tested. One of the most important test methods is the breaker timing test, which consists of measuring the mechanical operational time of the breakers contact within the VI tube. Timing tests in circuit breaker will always be important to prevent damages. Incorrect operation of circuit breaker can have of disastrous consequences on the equipment or the substation employees. Different measuring instrument can measure the operation times of a circuit breaker.

2. CONSTRUCTION AND MODE OF OPERATIONS

Component of circuit breaker

The major components of a vacuum circuit breaker are;

a. Control system

b. Operating mechanism

c. Mechanical linkage

d. Interrupter

2.1 Control system:

Anti Pumping feature: The anti-pumping relay is a device in circuit-breaker whose function is to prevent multiple breaker closures. For instance, if the operator gives the closing command to the breaker by pressing the close button and the breaker closes. However, a fault in the system causes the breaker to trip. Since the close command is still in the pressed condition, there is a chance of the breaker closing again and being tripped by the relay multiple times. This can damage the closing mechanism of the breaker. The anti-pumping relay prevents this by ensuring that the breaker closes only once for one close command from the control panel.

2.2 Operating Mechanism:

Stored Energy Operating Mechanism: The stored energy operating mechanism of the vacuum circuit breaker is an

integrated arrangement of springs, coils and mechanical devices designed to provide a number of critical functions. The sufficient potential energy for close and open the contacts of the vacuum interrupters operation is stored in powerful closing, opening and contact pressure springs. These springs are normally charged automatically, but there are additional provisions for manual charging by means of direct mechanically unlatching the closing spring using hand lever. Automatic charging of closing spring is accomplished by a separate electrical DC motor through gear train, which is bolted in operator housing and for manual charging a ratchet and pawl mechanism are employed. Closing spring is connected on one side of arming link and other to the main driving shaft of the opening spring mechanism, itself linked to the other mechanism such as cam and follower, electrical switches, latching. The operating kinematic mechanism is comprised of the electrical and mechanical components. All these functions are operated automatically through electrical charging motor, cutout switches, anti pumping relay, close coil, open coil, and auxiliary switch.

The circuit-breaker operating mechanism is a stored-energy spring mechanism. The force is transmitted from the operating mechanism to the pole assemblies via operating levers. The closing spring can be charged either electrically or manually, and latches automatically in when charging is complete. The closing spring acts as a stored-energy mechanism.

2.3 Mechanical Linkage:

Insulated operating kinematic linkages transmit the energy from the operating mechanism to the low voltage cabinet to the moving contact of the vacuum interrupter.

Four bar mechanism: It consists of four linkages each of them forms a turning pair and is connected in such a way that, whose relative motion is completely or successfully constrained. According to grashof's low of four bar mechanism, sum of largest and shortest link length should not be greater than the sum of other two link length if there is a continues relative motion between them. Position analysis, Velocity analysis and dimensional synthesis is begins with formulating the loop-closure equation for the four bar mechanism which helps to determining the toque arm and angle of rotation of kinematics. For optimum contact gap in vacuum interrupter, kinematic inversions are arranged precisely [9].

Spatial RSSR mechanism:

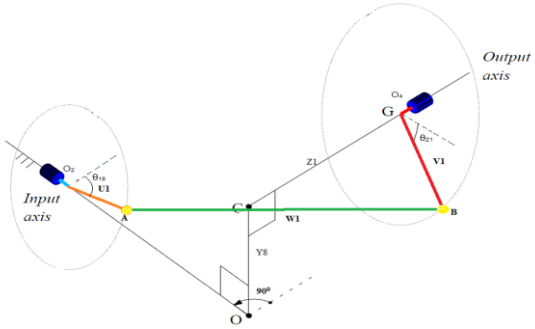

The RSSR spatial mechanism is one of the most popular mechanism for the motion transmission between two skew shafts (called input and output shafts for 90 degree change over mechanism) with a given relative pose (position and orientation). S and R are stands for spherical and revolute pairs respectively in spherical end jointed coupler.

The spatial RSSR mechanism has four binary links; the driving link is coupled to the cam operated intermediate shaft and the coupler W1 through a revolute and a spherical pair respectively. The spherical type coupler is then connected to the follower (i.e air side lever) by a spherical pair, and the follower is connected to the output shaft through a revolute pair which is common shaft for airside and gas side lever. Disregarding the rotation of the coupler about the axis defined by the two sphere pair centers, the mechanism has one degree of freedom. Depending on the link proportions different type of motion can obtained, the motion can be crank-and-rocker/double-rocker, drag-link. It converts a rotation about one axis into a rotation about a second axis within the housing, with a given variable transmission ratio[1].

2.4 Vacuum interrupter:

The opening and closing operations of current carrying contacts and associated arc interruption takes place in cylindrical vacuum chamber in the breakers which is called vacuum interrupter. Vacuum is used as a working medium for arc quenching in vacuum interrupter. The interrupter consist of two primary contacts one is fixed contact and another is movable contact. One pole of power supply is connected to the

stationary contact of vacuum interrupter at head side and another pole is connected to the movable contact at bottom with driving mechanism of the circuit breaker. The metal bellows provide a secure seal around the movable contact, preventing loss of vacuum while permitting vertical motion of the movable contact [10].

3. MATHEMATICAL MODEL AND TRANSFER FUNCTION

3.1 Assumptions and Sign Conventions

1) All angles are measured from positive X axis in anticlockwise direction
2) For vector the angle is always measured at the tail of the vector from positive X axis in anti-clockwise direction
3) The XY plane is the plane looking from right side of the breaker
4) YZ plane is plane looking from front side of the breaker
5) For four bar calculation the origins are moving as per contention for calculation(As per the known vectors)
6) The four bar analysis is done most by vector method
7) In case of the spring mechanism only the coordinates of the points are calculated to find the length of the spring
8) The mean stiffness as per the spring drawing is used for calculation of the force and torque, variation of the stiffness or forces mot considered
9) No friction is taken into consideration, all calculation is done only in static equilibrium positions over the travel of the cam during closing

The operating mechanism includes the kinematic inversion of four bar mechanism and spatial RSSR mechanism to control circuits and the components at system voltage. The on-site testing practices include timing, travel and contact force measurements to assess the integrity of the kinematic chain and control circuits

3.2 Four Bar Mechanism:

Transfer function for mathematical model is described in below section,

The loop closure equation simply sums the position vectors around the complete four-bar linkage, and in vector form is given by,

I1+L4-G1-H1=0…….…… (3.1)

Each link has length L and is at angle θ; hence the complex form may be written as

$I_1e^{i\theta} + L_2e^{i\theta} - G_3e^{i\theta} - H_4e^{i\theta} = 0$

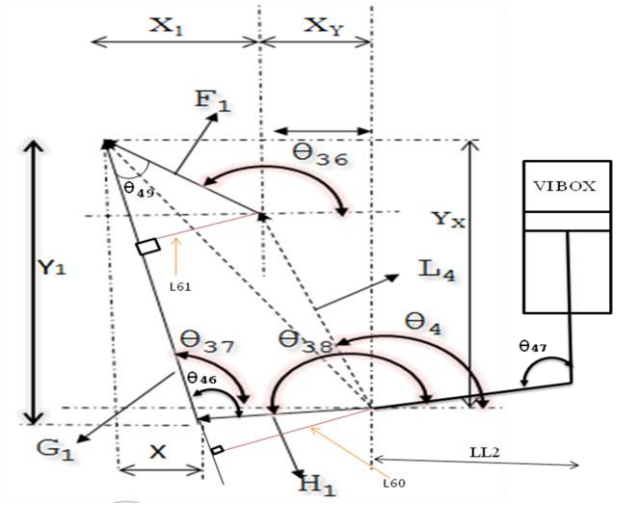

Figure 3.1: Four bar mechanism.

We can expand (Eq.4.28) using Euler's identity, then separate Real and Imaginary terms.

$L_4 *COS\theta_4 + I_1*COS\theta_{36} = G_1*COS\theta_{37} + H_1* COS\theta_{38}$

$L_4 *SIN\theta_4 + I_1*SIN\theta_{36} = G_1*SIN\theta_{37} + H_1* SIN\theta_{38}$

Let, $X = L_4 *COS\theta_4 + I_1*COS\theta_{36} = L43$

$Y = L_4 *SIN\theta_4 + I_1*SIN\theta_{36} = L44$

Hence, $G_1*COS\theta_{37} + H_1* COS\theta_{38} = X$

$G_1*SIN\theta_{37} + H_1* SIN\theta_{38} = Y$

Solving For θ6

$H_1* COS\theta_{38} = X - G_1*COS\theta_{37}$ …… (3.2)

$H_1* SIN\theta_{38} = Y - G_1*SIN\theta_{37}$ …… (3.3)

Squaring and adding (3.2) and (3.3),

$H_1^2 = X^2 + Y^2 + G_1^2 - 2*G_1*X*COS\theta_{37} - 2*G_1*Y*SIN\theta_{37}$

Hence

$X*COS\ \theta_{37} + Y*SIN\ \theta_{37} = (X^2 + Y^2 + G_1^2 - H_2^2)/(2*G_1)$

Let $C = (X^2 + Y^2 + G_1^2 - H_2^2)/(2*G_1) = L45$

By solving, we get single quadratic equation with one unknown θ_{37},

$X*COS\ \theta_{37} + Y*SIN\ \theta_{37} = C$……..…. (3.4)

Solution for Eq.4.31 is derived in appendix 2,

Therefore,

$\theta_{37} = TAN\text{-}1(Y/X) \pm TAN^{-1}(SQRT(X^2 + Y^2 - C^2)/C)$

Solution for θ_{38},

3.3 By Displacement Equation for Four Bar Mechanism

Consider a planar four bar linkage (fig.4.12).this linkage is characterized by four revolute with parallel axes, the distance between successive axes being parameters F1,G1 L1,H1. The Kinematic synthesis of four bar linkage will yield an approximation to a desired function between input and output angles.

In this section algebraic method for synthesis of four bar linkage mechanism is considered. Such method of synthesis is based on displacement equation, i.e. equation relating the input and output variable of a mechanism in terms of its fixed parameters.

Displacement equation of the four bar linkage may be obtained by considering the rectangular coordinate system (fig.4.11) with respect to which coordinates of A,B may be written as follows,

From figure 3.1,

$F_1 * COS\ \theta_{36}=X_1$

$F_1 * SIN\ \theta_{13} = Y_1$

$L_4 * COS\ \theta_4 = X_Y$ ……. (3.5)

$L_4 * SIN\ \theta_4 = Y_X$

Since distance AB is fixed and equal to G1, application of Pythagoras theorem yields,

$Y^2 + X^2 = G_1^2$

With reference to figure 4.12,

$(-Y_1+ Y_X+Y_2)^2 + (X_1- X_Y- X_2)^2 = G_1^2$

…….(3.6)

Substituting Eq.3.5 into Eq.3.6,

$(-Y_1+ Y_X + (H_1* SIN\ \theta_{38}))^2 + (X_1- XY - (COS\ \theta_{38}* H_1)^2 = G_1^2$

$(A+ H_1* SIN\ \theta_{38})^2 + (B-(COS\ \theta_{38}* H_1))^2 = G_1^2$

Consider, $A = Y_X - Y_1$ and $B = X_1 - X_Y$

$A^2 + B^2 + H_1^2 - G_1^2 + (2 * A* H_1* SIN\ \theta_{38}) - (2 * B * H_1 * COS\ \theta_{38}) = 0$

$(2 * A* H_1 * SIN\ \theta_{38}) - (2 * B * H_1* COS\ \theta_{38}) = -A^2 - B^2 - H_1^2 + G_1^2$

$A* SIN\ \theta_{38} - B\ COS\ \theta_{38} = (- A^2 - B^2 - H_1^2 + G_1^2) / (2 * H_1)$

After trigonometric simplification this may written as,

$A* SIN\ \theta_{38} - B\ COS\ \theta_{38} = C$……..(3.7)

Where the coefficients are,

$A = Y_X - Y_1$

$B = X_1 - X_Y$

$C = (-A^2 - B^2 - H_1^2 + G_1^2) / (2 * H_1)$

Equation 3.7 may be solved for displacement analysis of the four bar linkage. That is, θ_{38} is found explicitly as a function of θ_{36} and parameters F1,G1 L1,H1. Such a solution is obtained by equation (3.8) in terms of TAN ($\theta_{38}/2$).

We have only one unknown, θ_{38}. A standard technique for dealing with this is to use the identities

$SIN\theta_{38} = \frac{2\tan\frac{\theta_{21}}{2}}{1+\tan^2\frac{\theta_{21}}{2}}$ and $COS\ \theta_{38} = \frac{1-\tan^2\frac{\theta_{21}}{2}}{1+\tan^2\frac{\theta_{21}}{2}}$

……...(3.8)

Substituting these in to equation (3.7) and multiplying by the common denominator, we get a single quadratic equation in one unknown, $\tan\frac{\theta_{21}}{2}$.

$2A*\tan(\theta_{38}/2)+B(1- \tan^2(\theta_{38}/2))=C*(1+ \tan^2(\theta_{38}/2))$

That can solve by using equation,

$$\tan(\theta 38/2) = \frac{A \pm \sqrt{A^2+B^2-C^2}}{B+C}$$

Therefore,

$\theta_{38} = TAN\text{-}1(A / -B) \pm TAN^{-1}(SQRT(A^2 + B^2 - C^2) / C)$……(3.9)

Also solved by using method 1 (eq.)

$\theta_{38} = TAN^{-1}((Y - G_1* SIN\theta_{37})/(X - G_1* COS\theta_{37}))$……..……(3.10)

3.4 Calculation for Four Bar Mechanism For Torque Arms.

Torque arm for contact system four bar mechanism is obtained by considering minimum 8mm contact gap between the contacts.

a. θ_{49} = Angle for calculation of Torque arm on operating shaft for force from contact spring.

If $L_{49} <= 8$ then $\theta_{49} = 180-\theta_{42} +180+\theta_{40}$ …… (3.11)

Else $\theta_{49} = 180-\theta_{45} + 180 +\theta_{40}$

Angle for calculation of torque arm for contact spring on rocker

If L_{49} <=8 then θ_{46}= 0, else

$\theta_{46}= \theta_{45} +180 -\theta_{41}$ …….…..…. (3.12)

Torque arm length Force from contact spring on rocker

$L_{57} = LL_4*SIN\theta_{46}$

If L_{49} <=8 then $\theta_{49}= 180-\theta_{42} +180+\theta_{40}$ ……(3.13)

Else $\theta_{49}= 180-\theta_{45} + 180 +\theta_{40}$

Angle for calculation of torque arm for contact spring on rocker

If L_{49} <=8 then θ_{46}= 0, else

$\theta_{46}= \theta_{45} +180 -\theta_{41}$ …….…..…. (3.14)

Torque arm length Force from contact spring on rocker

$L_{57} = LL_4*SIN\theta_{46}$

Angle for Torque arm for force from spring to eye bolt

If L_{49} <=8 then θ_{47} = 0, Else

$\theta_{47} = 180 - \theta_{41} + LL5 +90$,

Torque arm for force from spring to eye bolt

$L_{58} = LL_2* SIN\theta_{47}$ ……. (3.15)

Torque arm for torque from contact spring on kinematic shaft

$L_{59} = I_1* SIN\theta_{49}$…….…… (3.16)

Angle for torque arm calculation for force on gas side coupler from kinematic shaft, from figure:3.1.

$\theta_{50} = \theta_{37} -(180 + \theta_{38})$ …… (3.17)

Torque arm calculation for force on gas side coupler from kinematic shaft,

$L_{60} = H_1* SIN\theta_{50}$…….…… (3.18

Angle for torque from coupler force on gas side to lever gas side, from figure: 3.1,

$\theta_{51} = 180-\theta_{37} -(180 - \theta_{36})$ ……..…(3.19)

Torque arm calculation for force on gas side coupler from kinematic shaft

$L_{61} = H_1* SIN\theta_{51}$

The energy margin is considered in this case by the torque margin available i.e. graph is plotted for the torque on the moving arm due the force from the closing springs and opposing torque coming from the contact system (figure5.3). If the torque coming from the contacts system is more at some instance than the torque coming from the closing springs the breaker may not close. So the mathematical model for force and torque from contact springs are generated and optimized as shown in figure 4.16.

$F_{contact}$ = Contact force

$\boldsymbol{\tau_1}$ =Fcs*L57 …….……(3.20)

$F_{contact} = \boldsymbol{\tau_1/L58}$

τ_2 = Fcs*L59…….……..…...(3.21)

$F_1 = \boldsymbol{\tau_2 /L60}$

$\boldsymbol{\tau_3} = F_1$ * L61…….(3.22)

3.5 RSSR Spatial Mechanism

In spatial mechanism driving link U1 is coupled with a cam operated intermediate shaft and the coupler W1 through a revolute and a spherical pair respectively. The spherical joint type coupler is then connected to the rotary bushing (i.e air side lever) by a spherical pair, and the follower is connected to the output shaft through a revolute pair which is common shaft for airside and gas side lever [1].

With reference to Figure 4.6, A and B are the centers of the spherical joints and describe two circles centered respectively at points O_2 and O_4, which belong to the input and output axes respectively. The Vector Y_8 represents the minimum distance between the input and output axes.

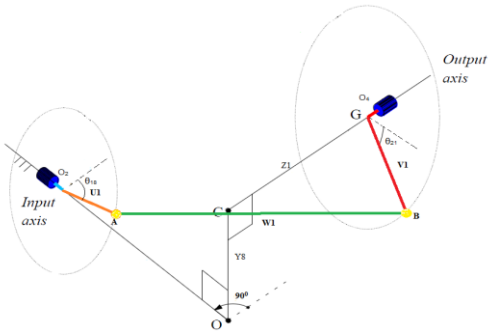

Figure 3.2 : RSSR spatial mechanism [2]

The mechanism parameters are defined as follows [2]:

a. U_1, driving link (link 1) length, i.e. the distance of point A from the O_2 ,input axis.

b. W_1, coupler link (link 2) length, i.e. the distance between points A and B;

c. V_1 follower link (link 3) length, i.e. the distance of point B from the O_4, output axis.

d. $\mathbf{Y_8} = |\mathbf{Y_8}|$, minimum distance between the input and output axes;

e. $X_8 = |X_8|$, distance between points O_2 and ProjO_4;

f. $Z_1 = |Z_1|$, distance between points O_4 and ProjO_2;

g. θ_{18}, input link angle about **O_2** measured according to the right-hand rule from the perpendicular direction;

h. θ_z=0 angular offset: angle between the axes of the revolute pairs measured about perpendicular direction according to the right-hand rule from the output revolute axis;

i. θ_{21}, output link angle measured about O_4 according to the right-hand rule from the perpendicular direction.

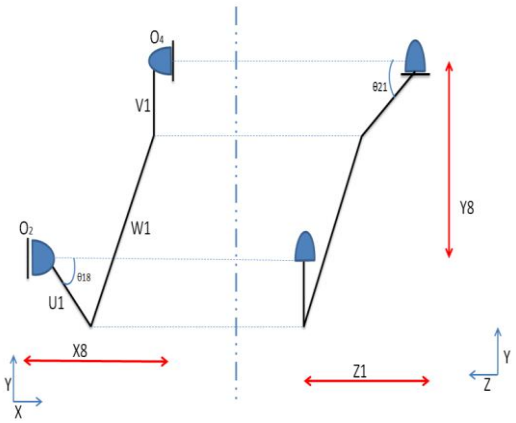

Figure 3.3 : 2D View for RSSR spatial mechanism

The development begins with the loop closure equation for a spatial mechanism, as shown in Figure 4.7,

From the Vector Loop closer equation is, -

$RO4O2+RO2U+RUV-RO4V=0$…….. (3.23)

Vector for each link is given by,

$RO_4O_2=X_8\,i + Z_1\,k - Y_8\,j$

$RO_2U=U_1*\cos(\theta_{18})i+U_1 \sin(\theta_{18})\,j$

$RUV=R_1\,i + R_2\,j + R_3\,k$ …….. (3.24)

$RO_4V=-V_1 \sin(\theta_{21})\,j + V_1 \cos(\theta_{21})\,k$

$R_1\,i$, $R_2\,j$, $R_3\,k$ are the components of the spatial vector **W_1**.

Substituting Eq.4.18 into Eq.4.17 gives,

$X_8\,i + Z_1\,k - Y_8\,j+(U_1\cos(\theta_{18})i+U_1 \sin(\theta_{18})j)+R_1\,i + R_2\,j + R_3\,k-(-V_1 \sin(\theta_{21})\,j + V_1 \cos(\theta_{21})\,k)=0$

On separating this into its i, j, k components and rearranging, we get the following three equations:

$R_1\,i = (-U_1\cos\theta_{18})+X_8$

$R_2\,j = (U_1\sin\theta_{18})+Y8-(V1\sin\theta_{21})$ …… (3.25)

$R_3\,k = -Z_1-(V_1\cos\theta_{21})$

Next we can square and add Eq.4.19 and remembering that Ruv=267 mm

$(X_8^2+(-U_1\cos\theta_{18}))^2 + (Y_8-(U_1\sin\theta_{18}+V_1\sin\theta_{21}))^2 +(-Z_1-V_1\cos\theta_{21})^2 = W_1^2$

$X_8^2+(U_1\cos\theta_{18})^2-2X_8U_1\cos\theta_{18}+Y_8^2-2U_1Y_8\sin\theta_{18}-2Y_8V_1\sin\theta_{21}+(U_1\sin\theta_{18})^2+(V_1\sin\theta_{21})^2+2U_1\sin\theta_{18}V_1\sin\theta_{21}+Z_1^2+2Z_1V_1\cos\theta_{21}+(V_1\cos\theta_{21})^2=W_1^2$

So the input angle θ_{18} and the output angle θ_{21} as shown in figure 4.7 are related by equation,

$X_8^2+U_1^2+Y_8^2+V_1^2+Z_1^2-W_1^2-2X_8U_1\cos\theta_{18}-2U_1Y_8\sin\theta_{18}+\sin\theta_{21}(-2Y_8V_1+2U_1V_1\sin\theta_{18})+\cos\theta_{21}(2Z_1V_1)=0$

$\sin\theta_{21}(-2Y_8V_1+2U_1V_1\sin\theta_{18})+\cos\theta_{21}(2Z_1V_1)=-(X_8^2+U_1^2+Y_8^2+V_1^2+Z_1^2-W_1^2-2X_8U_1\cos\theta_{18}-2U_1Y_8\sin\theta_{18})$…… (3.26)

Eq.3.26 is written as,

$A\sin\theta_{21}+B\cos\theta_{21}=C$

Where the coefficients are,

$A=(2Y_8V_1-2U_1V_1\sin\theta_{18})$

$B=-(2Z_1V_1)$

$C=(X_8^2+U_1^2+Y_8^2+V_1^2+Z_1^2-W_1^2-2X_8U_1\cos\theta_{18}-2U_1Y_8\sin\theta_{18})$

$$\theta_{21}=\tan^{-1}\frac{B}{A}\pm\tan^{-1}\frac{\sqrt{A^2+B^2-C^2}}{C} \quad \text{…… (3.27)}$$

Eq. 4.21 gives the Angle of the lever on rotary bushing

For the analysis of 3D kinematic the analysis in XY plane first and then in YZ plane with an assumption that the center point of the spherical bearing will be in the same X location while the lever on rotary bushing is rotating, as shown in figure 4.8. Now by considering coupler projection w.r.t 90 degree change over mechanism,

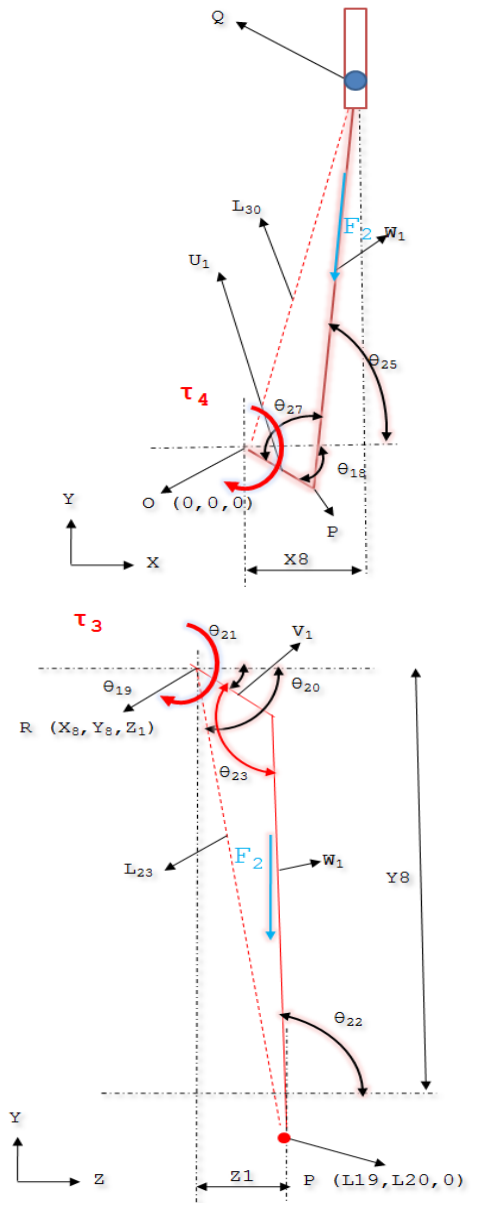

Figure 3.4 : Spatial mechanism in two plane (XY and YZ Plane)

Let W_p= Coupler projection length

=L20+(Y8-(-V1*SIN θ_{21})…… (4.22)

Assume

P = center point of spherical bearing on the intermediate shaft lever

Q = Center point of the spherical bearing on the lever on rotary bushing

O = Origin

R = Point on the axis of rotary bushing shaft in same Y location of Coordinate of point P

From figure 4.8

L_{19} =X coordinate = U_1*COSθ_{18}

L_{20} =Y coordinate = U_1*SINθ_{18}

Z coordinate = 0

Coordinates of Point Q

X = X_8

Y= to be found out

Z = to be found out

Coordinates of point R

X = X_8

Y = Y_8 (See YZ Plane)

Z = Z_1 (See YZ Plane)

Length of line joining Point P and Point R in YZ plane

L_{23} = SQRT ((L_{20}-Y_8)^2+(0-Z_1)^2)

Angle for Line joining point P and point R in YZ plane

θ_{19} = tan-1((L_{20}-Y_8)/(0-Z_1))

θ_{20} = 180+ θ_{19}

θ_{23} = θ_{21}+θ_{22}

Torque arm for torque from Rotary Bushing lever

L_{27} = V_1* SIN θ_{23} ……(4.23)

In x-y plane

Coordinates of point Q

L_{28} = X_8 =X coordinate = L30*COSθ_{24}

L_{29} = V_1* SIN θ_{21} + Y_8=Y coordinate = L_{30}*SINθ_{24}

Line joining point q and origin

L_{30} = SQRT (L_{28}^2+L_{29}^2)

Now writing the vector equations

Here we are rechecking the travel by calculating θ_{26} which is equal to θ_{18}

$U_1e^{i\,\theta 17} + W_pe^{i\theta 25} = L_{30}e^{i\theta 24}$ …….. (3.28)

We can expand (3.28) using Euler's identity, then separate Real and Imag terms.

U_1*COSθ_{17} + W_P*COSθ_{25} = L_{30}*COSθ_{24}

U_1*SINθ_{17} + W_P*SINθ_{25} = L_{30}*SINθ_{24}

X = L_{30}*COSθ_{24}

Y = L_{30}*COSθ_{24}

U_1*COSθ_{17} + W_P*COSθ_{25} =X

U_1*SINθ_{17} + W_P*SINθ_{25} =Y

U_1*COSθ_{17} = X - W_P*COSθ_{25}…… (3.29)

$U_1*SIN\theta_{17} = Y - W_P*SIN\theta_{25}$……..… (3.30)

Squaring and adding

$U_1^2 = X^2 + Y^2 + W_P^2 - 2*X*W_1*COS\ \theta_{25} - 2*Y*W_1*SIN\theta_{25}$

$L_{24}*COS\ \theta_{25} + L_{25}*SIN\theta_{25} = (L_{24}^2 + L_{25}^2 + V_1^2 - W_P^2)/(2*V_1)$

Let $(X^2 + Y^2 + U_1^2 - W_P^2)/(2*W1) = C$……. (3.31)

Hence,

$X*COS\ \theta_{26} + Y*SIN\ \theta_{26} = C$

Solution for θ_{25} is,

$\theta_{25} = TAN^{-1}(Y/X) \pm TAN^{-1}(SQRT(X^2 + Y^2 - C^2)/C)$

From figure 4.8,

$\theta_{23} = \theta_{21} + \theta_{22}$……..(3.32)

Eq. 3.32 gives Angle for calculating the force on coupler from the lever on rotary bushing in air.

Torque arm for force on coupler from lever on rotary bushing.

$L_{27} = V_1 * SIN\ \theta_{23}$ ……..(3.33)

$\theta_{27} = 180 - \theta_{25} + \theta_{18}$……..……..….(3.34)

Torque arm for torque on intermediate shaft

$L_{32} = U_1 * SIN\ \theta_{27}$ ……..……..… (3.35)

τ_3 = Torque from contact spring on Rotary bushing

$F_2 = \tau_3/L_{27}$ = Force on coupler from rotary bushing lever

$\tau_4 = F_2*L_{32}$ = Torque on intermediate shaft from contact spring

4. RESULTS AND DISCUSSION

As per the previous discussion and the various issues that were taken into consideration, transfer functions were developed for each of it. Sensitivity analysis was done. And the critical dimensions were found out. The objective function was optimized.

4.1Energy margin results:

The difference in the energy between the closing springs and energy required to close the breaker against the contact spring force. The energy margin should always be positive during each step of closing. The energy margin is considered in this case by the torque margin available i.e. graph is plotted for the torque on the moving arm due the force from the closing springs and opposing torque coming from the contact system(fig 4.1). If the torque coming from the contacts system is more at some instance than the torque coming from the closing springs the breaker may not close. Energy margin during closing and opening (Static) to decide the spring forces required for our mechanism.

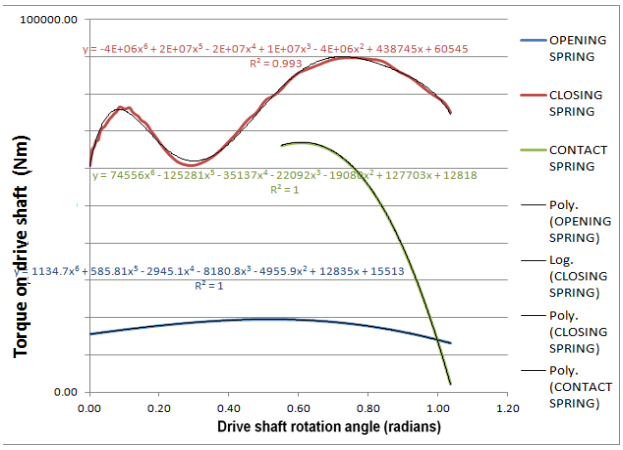

Figure 4.1: Graph of torque vs drive shaft angle

Results from Excel based static force analysis

Closing spring energy:

Table 4.1: Closing spring Energy

Closing spring energy					
y = -4E+06x6 + 2E+07x5 - 2E+07x4 + 1E+07x3 - 4E+06x2 + 438745x + 60545					
R² = 0.993					
			0		
Intercept	60545.34		1.11		
X	438744.7		84869.02385		
X2	-4095730		84.86902385	Nm or J	
X3	14082616		Energy from closing spring		
X4	-2.2E+07				
X5	15915197				
X6	-4440924				

Opening spring energy

Table 4.2: Opening spring Energy

Opening spring energy					
y = 1134.7x6 + 585.81x5 - 2945.1x4 - 8180.8x3 - 4955.9x2 + 12835x + 15513					
R² = 1					
Intercept	15513.21		0		
X	12834.58		1.04		
X2	-4955.91		18444.0803		
X3	-8180.78		18.4440803	Nm or J	
X4	-2945.06				
X5	585.8109		Opposing energy from opening spring		
X6	1134.739				

Contact spring energy

Table 4.3: Contact spring Energy

Contact spring energy					
y = 74556x6 - 125281x5 - 35137x4 - 22092x3 - 19080x2 + 127703x + 12818					
R² = 1					
Intercept	12817.51		0.05		
X	127702.8		1.12		
X2	-19079.9				
X3	-22091.6		45972.92569	46772.5978	
X4	-35136.8		45.97292569	Nm or J	
X5	-125281		Opposing energyg from Contact sppring		
X6	74556.37				

Energy margin

Table 4.1: Total energy margin

	64.41	Total opposing energy	
Extra energy	1.317	Ratio of input energy to opposing energy	
	0.317		
We have	32%	Extra energy	

4.2 Contact Force Measurement

Results from Excel based static force analysis

Table 4.5: Contact force measurements

Theoretical contact force (N)	Actual contact force (N)						
Excel based calculation	using dimensional parameter				measuring setup		
		L1	L2	L3	L1	L2	L3
	L0	78	78	78			
2670.808628	K	43.05	43.05	43.05	2586.8	2475.2	2486.8
	Spring force	1155	1076	1096			
	Leverage	2.25	2.25	2.25			
	Contact force	2599.79	2421.563	2468.057			

Using dimensional parameter

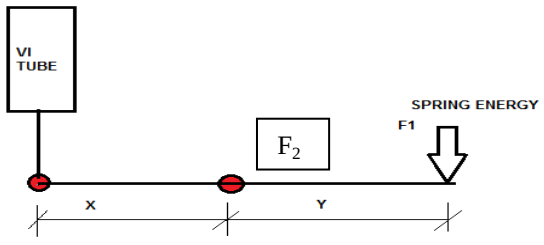

b. Figure 4.2: Contact force measurements

4.3 Operational characteristics Results:

Table 4.6: Operational characteristics calculations

Description	Unit	**Excel based** Measured parameters	Actual Measured parameters
Rotation angle of breaker shaft in VIBOX [°]	°	80	73
Rotation angle of rotary bushing shaft in VIBOX [°]	°	78	72
Rotation angle of intermediate shaft in drive [°]	°	64	59

Closing	unit	**Excel based** Measured parameters	Actual Measured parameters
Angular velocity of closing	°/ms	3.1701	4.57
Closing Contact Time	**millisecond**	43.0698	45

Opening	unit	**Excel based** Measured parameters	Actual Measured parameters
Angular velocity of opening	°/ms	3.48	4.41
Opening Contact Time	**millisecond**	29.2	31

For validating the theoretical result the measurement for the Vacuum circuit breaker measured in practically is tabulated in above. The transfer function developed for Theoretical calculations compares the change in force due to dimensional variations in mechanism. Also compares the practical values on standard measuring instrument.

5. CONCLUSION

From the above discussion the gain from the project are the ways to analyze the complex optimization problem having many optimization parameters. The excel solver is used to solve the optimization problem. As per calculations we have 32% more energy in the closing spring which should be sufficient enough to overcome the friction, tolerance and inertia of the additional parts in the circuit breaker system. The calculation for the energy margin between the closing springs and the contact system springs showed that the force coming from the contact system is less than the force given by the closing mechanism. Thus the mechanism is suitable for breaker operations.

For validating the theoretical result the contact force for the Vacuum circuit breaker measured in practically is tabulated in table: 4.5. There is 05% variation in the theoretical and practical values. The transfer function developed for Theoretical contact force compares the change in force due to dimensional variations in mechanism. Also compares the practical values on standard measuring instrument. Measurement is considered in two locations, one is breaker in contact close position and another is in contact open position (i.e. upper and lower) which is depends upon the continuity of contact with VI tubes.

Results from excel based calculation and actual measured are comparable. Form Operational characteristics measurement there is a 09% variation in the theoretical and practical values. The deviation in the results is due to the absence of dampers friction, tolerance, inertia force etc. The maximum velocity of the moving contact is 3.17 m/s and the obtained values are within the limit.

REFERENCES

[1] Synthesis of four-bar linkage using displacement equations, Annals of the University of Petroşani, Mechanical Engineering, 12 (2010).

[2] Synthesis of the optimal RSSR mechanism for the motion transmission between skew axes with variable pose, Claudio Mazzotti1, Marco Troncossi1, Vincenzo Parenti-Castelli11 Department of Engineering for Industry, University of Bologna, Italy.

[3] Synthesis of kinematic linkages book by goldstein, hartenberg andkeler M L (1959).

[4] SION Vacuum Circuit-Breakers 3AE5 and 3AE1 Medium-Voltage Equipment · Catalog HG 11.02 · 2013

[5] Vacuum Circuit Breaker Operator Module © 2001 Siemens Energy, Inc.

[6] "Algebraic method of synthesis Using displacement equations", chapter 10. ASME J. Eng,Vol 81(1959).

[7] VD4/R MV vacuum circuit-breakers for secondary distribution, by ABB © Copyright 2013 ABB

